

## Accepted Manuscript

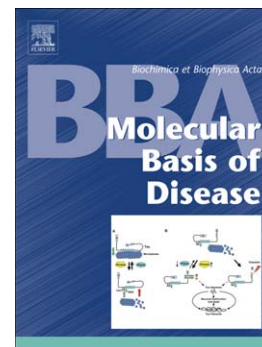
Defects in mitochondrial energetic function compels Fanconi Anemia cells to glycolytic metabolism

Enrico Cappelli, Paola Cuccarolo, Giorgia Stroppiana, Maurizio Miano, Roberta Bottega, Vanessa Cossu, Paolo Degan, Silvia Ravera

PII: S0925-4439(17)30084-4  
DOI: doi:[10.1016/j.bbadis.2017.03.008](https://doi.org/10.1016/j.bbadis.2017.03.008)  
Reference: BBADIS 64714

To appear in: *BBA - Molecular Basis of Disease*

Received date: 9 November 2016  
Revised date: 9 March 2017  
Accepted date: 13 March 2017



Please cite this article as: Enrico Cappelli, Paola Cuccarolo, Giorgia Stroppiana, Maurizio Miano, Roberta Bottega, Vanessa Cossu, Paolo Degan, Silvia Ravera, Defects in mitochondrial energetic function compels Fanconi Anemia cells to glycolytic metabolism, *BBA - Molecular Basis of Disease* (2017), doi:[10.1016/j.bbadis.2017.03.008](https://doi.org/10.1016/j.bbadis.2017.03.008)

This is a PDF file of an unedited manuscript that has been accepted for publication. As a service to our customers we are providing this early version of the manuscript. The manuscript will undergo copyediting, typesetting, and review of the resulting proof before it is published in its final form. Please note that during the production process errors may be discovered which could affect the content, and all legal disclaimers that apply to the journal pertain.

# DEFECTS IN MITOCHONDRIAL ENERGETIC FUNCTION COMPELS FANCONI ANEMIA CELLS TO GLYCOLYTIC METABOLISM.

Enrico Cappelli<sup>1</sup>, Paola Cuccarolo<sup>#2</sup>, Giorgia Stroppiana<sup>3</sup>, Maurizio Miano<sup>1</sup>, Roberta Bottega<sup>4</sup>,  
Vanessa Cossu<sup>5</sup>, Paolo Degan<sup>2\*</sup>, Silvia Ravera<sup>5\*</sup>.

<sup>1</sup>Hematology Unit, Istituto Giannina Gaslini, 16148 Genova, Italy; <sup>2</sup>U.O. Mutagenesis, IRCCS AOU San Martino – IST (Istituto Nazionale per la Ricerca sul Cancro), Genova, Italy; <sup>3</sup>Laboratorio Diagnosi Pre e Postnatale Malattie Metaboliche, Istituto Giannina Gaslini, 16148 Genova, Italy; <sup>4</sup>Institute for Maternal and Child Health – IRCCS Burlo Garofolo, Trieste, Italy; <sup>5</sup>Laboratorio di Biochimica, Dipartimento di Farmacia, Università di Genova, Genova, Italy.

\* These Authors have contributed equally to this work.

## Corresponding Author:

Dr. Paolo Degan,

U.O. Mutagenesis, IRCCS AOU San Martino – IST (Istituto Nazionale per la Ricerca sul Cancro),  
Largo Rosanna Benzi, 10 - 16132 Genova, Italy.

Phone: 0039 010 5558542

Fax: + 39 010 5558237

e-mail: paolo.degan@hsanmartino.it

<sup>#</sup> Actual address: IRCCS Mario Negri, Villa Camozzi, V. G.B. Camozzi, 3, 24020 Bergamo

## ABSTRACT

Energetic metabolism plays an essential role in the differentiation of haematopoietic stem cells (HSC). In Fanconi Anaemia (FA), DNA damage is accumulated during HSC differentiation, an event that is likely associated with bone marrow failure (BMF). One of the sources of the DNA damage is altered mitochondrial metabolism and an associated increment of oxidative stress. Recently, altered mitochondrial morphology and a deficit in the energetic activity in FA cells have been reported. Considering that mitochondria are the principal site of aerobic ATP production, we investigated FA metabolism in order to understand what pathways are able to compensate for this energy deficiency. In this work, we report that the impairment in mitochondrial oxidative phosphorylation (OXPHOS) in FA cells is countered by an increase in glycolytic flux. By contrast, glutaminolysis appears lower with respect to controls. Therefore, it is possible to conclude that in FA cells glycolysis represents the main pathway for producing energy, balancing the NADH/NAD<sup>+</sup> ratio by the conversion of pyruvate to lactate. Finally, we show that a forced switch from glycolytic to OXPHOS metabolism increases FA cell oxidative stress. This could be the cause of the impoverishment in bone marrow HSC during exit from the homeostatic quiescent state. This is the first work that systematically explores FA energy metabolism, highlighting its flaws, and discusses the possible relationships between these defects and BMF.

**Keywords:** Fanconi Anaemia, energy metabolism, glycolysis, oxidative phosphorylation, oxidative stress, cancer-prone diseases.

**Abbreviations:** AML: acute myeloid leukaemia; AMPK: Adenosine Monophosphate-Activated Protein Kinase; Antimyc: antimycin A; BMF: bone marrow failure; DCA: dichloroacetate; H2DCF: 2',7'-dichlorofluorescein; H2DCFDA: 2',7'-dichlorodihydrofluorescein diacetate; HSC:

haematopoietic stem cells; FA: Fanconi Anaemia; G6PD: glucose 6-phosphate dehydrogenase; Gal: Galactose; HK: hexokinase; LDH: lactate dehydrogenase; MDA: malondialdehyde; MDS: myelodysplastic syndrome; MMD: mitochondrial membrane depolarisation; OXPHOS: oxidative phosphorylation; PDH: pyruvate dehydrogenase; PFK: phosphofructokinase; P/M: pyruvate + malate; ROS: reactive oxygen species; Rot: rotenone; Succ: succinate; TMRM: tetramethyl rhodamine;

## 1. INTRODUCTION

FA is an autosomal recessive disorder, characterised by aplastic anaemia, developmental delay, physical abnormalities and increased incidence of solid tumours and leukaemias [1,2]. The primary cause of death in FA patients is bone marrow failure, and about 80–90% of FA patients develop aplastic anaemia, which is often fatal. In addition, 20–25% of patients develop malignancies of myeloid origin, including acute myeloid leukaemia (AML; 36%) and myelodysplastic syndrome (MDS; 54%), among other cancers [3].

To date, around 18 genes are responsible for known complementation FA groups [4,5]. However, the highest mutation frequencies occur in three genes: FANCA (FA complementation group A), which accounts for the 65% of the mutation frequency, and FANCC and FANCG which share, respectively, the remaining 15% and 10% [6]. Moreover, notwithstanding that FA is characterised by a genetic complexity, a remarkably high clinical and cellular phenotype homology is shared among FA patients. The mutation of FA genes leads to a failure of DNA repair mechanisms, making cells sensitive to interstrand cross linkers, which induce cell cycle arrest in the G2 phase [7]. However, there is evidence that FA proteins have multiple other functions as they are also implicated in cytokine hypersensitivity and immune responses [8,9].

FA cells are also characterised by high levels of oxidative stress and defective aerobic metabolism. In particular, FA cells are impaired in electron transport among Complexes I and III, while the oxidative metabolism through Complexes II, III and IV works properly and is indeed slightly improved with respect to controls [10,11]. However, considering that the mitochondrial pathway composed of Complexes I, III and IV is the principal source of the proton gradient [12] necessary for the oxidative ATP synthesis, the deficit in this pathway in FA determines a decrement in the ATP concentration and in the relative ATP/AMP ratio.

Moreover, the OXPHOS impairment is not the only mitochondrial damage in FA cells. In fact, mitochondrial localisation, morphology and integrity also appear altered [13], with spontaneous mitochondrial fragmentation.

Nevertheless, FA cells are able to produce the energy required to sustain cellular functions. In this work, we have investigated energetic metabolism in FA cells in order to understand what alternative pathways are involved in ATP production that are able to override the energetic defect. Our results show that FA cells mainly rely on glycolytic metabolism, while glutaminolysis is impaired. Moreover, the constrained reversion to OXPHOS could have a deleterious effect on cell fate.

## **2. MATERIALS AND METHODS**

### *2.1 Reagents*

All chemicals were purchased from Sigma Aldrich (St. Louis, MO, USA), unless otherwise indicated. Ultrapure water (Milli-Q; Millipore, Billerica, MA, USA) was used throughout. All other reagents were of analytical grade.

### *2.2 Cell lines and treatments*

Five Fanc-A Lymphoblast cell lines were obtained from the “Cell Line and DNA Biobank from Patients affected by Genetic Diseases” (G. Gaslini Institute) - Telethon Genetic Biobank Network (Project No. GTB07001) [14]. All five of these Fanc-A Lymphoblast cell lines were corrected with S11FAIN [15] retrovirus to generate the FA-corr cell lines. Two wild-type cell lines were also employed as controls. All cell lines were grown at 37°C in RPMI supplemented with 10% foetal calf serum and antibiotics. Treatments with rotenone (10  $\mu$ M), antimycin A (5  $\mu$ M), dichloroacetate (DCA, 25 mM), and galactose (Gal, 10 mM) were carried out for 24 h. After the treatment, the cells were harvested and used for protein extraction or biochemical experiments. Data

reported in this work are expressed as the mean  $\pm$  SD and are representative of at least five experiments conducted on five different Fanc-A Lymphoblast cell lines and relative controls.

### 2.3 Oxygen consumption measurements

Oxygen consumption was measured at 25 °C in a closed chamber, using an amperometric electrode (Unisense Microrespiration, Unisense A/S, Denmark). Cells were permeabilised with 0.03mg/ml digitonin for 1 min, centrifuged for 9 min at 1000 rpm and resuspended in the appropriate buffer. The same solution was used in the oxymetric measurements. For each experiment, 200,000 cells were used. 10 mM pyruvate plus 5 mM malate were added to stimulate the pathway composed by Complex I, III and IV. 20 mM succinate was added to stimulate the pathway formed by Complex II, III and IV. 0.1 mM rotenone or 50  $\mu$ M antimycin A, specific inhibitors of Complex I or Complex III, were used to block the first and the second pathway, respectively [10,16].

### 2.4 Cell homogenate preparation

Cultured cells were centrifuged at 1000 g for 2 min to remove the growth medium. The pellet was washed and resuspended in phosphate buffered saline (PBS) and sonicated twice for 10 seconds, with a break of 30 sec on ice, to prevent warming of the mixture, using the Microson XL Model DU-2000 (Misonix Inc, New York, NY, USA). The energy used to the treatment is around 0.44 kJ L<sup>-1</sup>. The efficacy of sonication was monitored using an optical microscope, with trypan-blue staining. Total protein content was estimated using the Bradford method [17].

### 2.5 Evaluation of ATP and AMP levels

ATP and AMP were measured according to the enzyme coupling method, following NAD(P)/NADP(H) reduction/oxidation at 340 nm.

Briefly, Perchloric acid (PCA; final concentration 2.5%) was added to 200.000 cells, to block all enzymes activities. The sample was centrifuged at 14000 rpm for 2 minutes and the supernatant was neutralized by the addition of  $K_2CO_3$  (final concentration 0.2 M).

For the ATP quantification assay was conducted on 50  $\mu$ l of neutralized supernatant in a medium contained: 100 mM Tris-HCl, pH 7.4, 5 mM  $MgCl_2$ , 50 mM glucose, 0.2 mM NADP. The assay started after the addition of 4  $\mu$ g of purified hexokinase and 2  $\mu$ g of glucose-6-phosphate dehydrogenase.

AMP concentration was assayed on 50  $\mu$ l of neutralized supernatant using the following medium: 100 mM Tris-HCl, pH 7.4, 5 mM  $MgCl_2$ , 10 mM phosphoenolpyruvate, 0.15 mM NADH, 0.2 mM ATP. The assay started after the addition of 4 $\mu$ g of purified pyruvate kinase plus lactate dehydrogenase and 2  $\mu$ g of adenylate kinase [10,16].

## 2.6 Glycolytic enzyme assays

Enzymatic activity was expressed as IU/mg of total protein (micromoles/min/mg of protein).

The reaction mixtures used for the determination of each enzyme activity were prepared as follows [18]. Hexokinase (HK, EC 2.7.1.1): 100 mM Tris-HCl pH 7.4, 5 mM  $MgCl_2$ , 200 mM glucose, 1 mM ATP, 0.91 mM NADP and 0.55 IU/ml of glucose 6 phosphate dehydrogenase (G6PD).

Phosphofructokinase (PFK, EC 2.7.1.11): 100 mM Tris-HCl pH 7.4, 2 mM  $MgCl_2$ , 5 mM KCl, 2 mM fructose 6 phosphate, 1 mM ATP, 0.5 mM phosphoenolpyruvate (PEP), 40  $\mu$ M rotenone, 0.2 mM NADH and 2 IU/ml of pyruvate kinase plus lactate dehydrogenase.

Pyruvate kinase (PK, EC 2.7.1.40): 100 mM Tris-HCl pH 7.6, 2.5 mM  $MgCl_2$ , 10 mM KCl, 0.6 mM phosphoenolpyruvate, 40  $\mu$ M rotenone, 0.2 mM NADH, 5 mM ADP and 1 IU/ml of lactate dehydrogenase.

Lactate dehydrogenase (LDH, EC 1.1.1.27): 100 mM Tris-HCl pH 9, 5 mM pyruvate, 40  $\mu$ M rotenone and 0.2 mM NADH.



### 2.7 TCA cycle enzyme assays

The activity of TCA cycle enzymes was measured in 25 µg of cell homogenate, using a double beam spectrophotometer (UNICAM UV2, Analytical S.n.c., Italy) at room temperature. Enzymatic activity was expressed as IU/mg total protein [18]. Reaction mixtures for each enzyme assay were as follows. Citrate synthase (EC 4.1.3.7): 100 mM Tris-HCl pH 8, 0.17 mM oxaloacetic acid, 0.2 mM acetyl-coA.  $\alpha$ -ketoglutarate dehydrogenase (EC 1.2.4.2): 100 mM Tris-HCl pH 7.5, 5 mM MgCl<sub>2</sub>, 40 µM rotenone, 2.5 mM  $\alpha$ -ketoglutarate, 0.1 mM CoA, 0.2 mM thiamine pyrophosphate, 3 mM NAD<sup>+</sup>, 0.1 mM CaCl<sub>2</sub>. fumarase (EC 4.2.1.2): 10 mM phosphate buffer pH 7.6 and 50 mM malate [18].

### 2.8 Western blot (WB) analysis

Denaturing electrophoresis [SDS-PAGE] was performed on 8–12 % gradient gels. 30 µg of protein was loaded for each sample. The follow antibodies were employed: anti phospho-AMPK (Thr 172) (Thermo Fisher Scientific Rockford, Illinois. US: cod: PA5-17831), anti AMPK (Thermo Fisher Scientific Rockford, Illinois. US: cod: PA5-29679) and anti-Actin (Santa Cruz Biotechnology, Santa Cruz, CA, USA; cod: sc-1616); all diluted 1:1000 in PBS. Secondary antibodies were from Sigma-Aldrich (St Louis, MO, USA). Protein molecular weight (MW) markers were supplied by Bio-Rad (Hercules, CA, USA). Quantitative densitometry was performed using a Chemi-Doc XRS plus instrument (Bio-Rad, Hercules, CA, USA).

### 2.9 Evaluation of malondialdehyde

To assess lipid peroxidation, the malondialdehyde (MDA) concentration was evaluated, using the thiobarbituric acid reactive substances (TBARS) assay [19]. This test is based on the reaction of MDA, a breakdown product of lipid peroxides, with thiobarbituric acid (TBA). The TBARS solution contained 15% trichloroacetic acid (TCA) in 0.25 N HCl and 26 mM thiobarbituric acid.

To evaluate the basal concentration of MDA, 600  $\mu$ l of TBARS solution was added to 50  $\mu$ g of total protein dissolved in 300  $\mu$ l of milliQ water. The mix was incubated for 40 min at 100°C.

Afterwards, the sample was centrifuged at 14000 rpm for 2 min and the supernatant was analysed spectrophotometrically, at 532 nm.

### 2.10 Evaluation of NADH/NAD<sup>+</sup> ratio

The NADH/ NAD<sup>+</sup> ratio was analysed in cell homogenates, using the “NAD/NADH Assay Kit (Colorimetric)” (Abcam, Cambridge, UK; cod: ab65348).

### 2.11 Glutaminase and glutamic dehydrogenase activity assay

Glutaminase activity was assayed in 30  $\mu$ g of sample homogenate, by following NAD<sup>+</sup> reduction at 340 nm. The assay mixture contained: 100 mM Tris-HCl pH 8.0, 50 mM Glutamine, 5 mM NAD<sup>+</sup>, 5 IU glutamic dehydrogenase.

Glutamic dehydrogenase was assayed in 30  $\mu$ g of sample homogenate, measuring the NADH oxidation at 340 nm. Assay mixture contained: 100 mM Tris-HCl pH 7.4, 20 mM  $\alpha$ -ketoglutarate, 0.22 M NH<sub>4</sub>Cl, 0.2 mM NADH and 1 mM ADP.

In both cases, 0.1 mM rotenone was added to inhibit the NADH oxidation from Complex I.

### 2.12 Mitochondrial membrane depolarisation (MMD) and oxidative stress induction (ROS)

After treatments, cells were washed and re-suspended in phosphate-buffered saline (PBS) and stained for 20 min at 37°C with 200 nM of tetramethyl rhodamine methyl ester (TMRM), to quantify mitochondrial membrane depolarisation (MMD), or stained with 2',7'-dichlorodihydrofluorescein diacetate (H2DCFDA) (all dyes from Thermo Fisher Scientific, Waltham, MA, USA), to quantify induced or basal reactive oxygen species (ROS). H2DCFDA is non-fluorescent compound, but inside cells it is cleaved to 2',7'-dichlorofluorescein (H2DCF), which, in the presence of oxidants, is finally converted to the fluorescent molecule DCF. Samples

were analysed on a CyAn ADP cytometer (Beckman Coulter, Mountain View, CA, USA) equipped with a 15-mW 488-nm argon ion laser. The plot of all physical parameters (forward scatter (FSC) versus side scatter (SSC)) was used to set the gate that delimits debris and aggregates. Ten thousand cells per sample were analysed. Data for MMD are presented as the percentage of cells that displayed depolarisation of the mitochondrial membrane after treatment of the cell lines with the various drugs. ROS data are presented as the percentage of the fluorescence increment induced by the various treatments in comparison with the ROS measured for untreated FANCA (10% offset)

### 2.13 Statistical analysis

Data were analysed using one-way ANOVA and unpaired two-tail Student's t tests using InStat software (GraphPad Software, Inc., La Jolla, CA, USA). Data are expressed as mean  $\pm$  standard deviation (SD) from three to five independent determinations performed in duplicate. In the figures SD are shown as error bars. An error probability with  $p < 0.05$  was regarded as significant.

## 3. RESULTS

### 3.1 Inhibitors and enhancers of OXPHOS activity do not induce significant changes in the energetic status of FA cells

Defects in oxidative metabolism have been described in FA cells [10,11]. In particular, an impairment in the electron transport from Complex I to Complex III has been reported, compromising the main source of cellular energy. To confirm that the metabolic defect in FA cells is really due to an impairment of electron transport among Complex I and Complex III, we evaluated the energetic status and oxygen consumption in the presence of drugs that stimulate or inhibit OXPHOS. Rotenone and antimycin A respectively inhibit Complex I and Complex III, while DCA or Gal enhance the oxidative energy metabolism. Specifically, DCA, inhibiting the activity of pyruvate dehydrogenase (PDH) kinase, induces an increment of PDH activity, favouring the

conversion of pyruvate to acetyl CoA and supplying the Krebs cycle [20]. On the other hand, galactose is considered as an alternative nutrient that is able to induce a great respiratory burst, bypassing glycolysis [21].

Figure 1, Panel A shows that the basal oxygen consumption (black columns) in FA cells is lower than that observed in Wt and FA-corr samples. Moreover, the addition of pyruvate + malate, which activates the pathway via Complexes I, III, and IV, determines an oxygen consumption increment only in Wt and FA-corr samples, confirming that this pathway is impaired in FA cells. By contrast, the increment of oxygen consumption induced by succinate is particularly high in FA compared with Wt and FA-corr (Figure 1, Panel A and Table I), suggesting that in FA the pathway composed by Complexes II, III and IV is very active, probably in order to compensate for the impairment of Complex I. These results were confirmed by the treatment with rotenone or antimycin A. In fact, only Wt and FA-corr cells are sensitive to this specific inhibitor of Complex I, while in the presence of antimycin A, oxygen consumption is impaired in all samples. When the OXPHOS activity is forced by the addition of DCA or Gal (Figure 1, panel B), the oxygen consumption induced by succinate increases in all samples, while the respiration after pyruvate + malate is enhanced only in Wt and FA-corr samples. Moreover, the impairment of aerobic metabolism in FA cells does not depend on an alteration in Krebs cycle. In fact, the activities of citrate synthase,  $\alpha$ -ketoglutarate dehydrogenase and fumarase are similar in FA cells and Wt and FA-corr cells (Figure 1, Panels C-E). This suggests that FA cells can potentially carry out the Krebs cycle, but the impairment of OXPHOS activity forces the metabolism through the anaerobic pathway.

The impairment of OXPHOS activity causes a lower energetic status in FA cells, as demonstrated by the reduced ATP/AMP ratio (Figure 2, Panel C). In particular, this unbalance seems due to decreased ATP production rather than increased AMP accumulation (Figure 2, Panels A and B, respectively). Genetic correction of FA cells (FA-corr) restored normal levels of ATP, AMP and ATP/AMP ratio (Figure 2, Panels A–C). Moreover, as expected, DCA and Gal induce an

increase in the ATP/AMP ratio in Wt and FA-corr cells, while in FA cells this increment was lower even though the oxygen consumption via the Complex II pathway was significantly increased. This may be because the energetic efficiency of the pathway through Complex II is lower than that of pathway through Complex I. In fact, the P/O ratio is roughly 2.5 when stimulated with pyruvate + malate and only 1.5 after the addition of succinate [22]. The addition of rotenone in the culture medium determines a reduction of ATP production and a consequent impairment of ATP/AMP ratio in Wt and FA-corrected samples, but not in FA cells. By contrast, antimycin A determines a reduction of the ATP/AMP ratio in all three samples, even though it was more evident in Wt and FA-corrected cells (about 80%) compared with FA cells (about 25%)(Figure 2, Panel C). Taken together, these data suggest that mitochondrial metabolism does not play a pivotal role in the energetic balance in FA cells.

### 3.2 AMPK hyper-phosphorylation drives FA cells to glycolytic metabolism

Reduction of ATP synthesis and AMP accumulation induce the activation of Adenosine Monophosphate-Activated Protein Kinase (AMPK), a sensor of the cellular energy state, which stimulates alternative catabolic processes to generate energy [23]. Therefore, considering the high AMP concentration in FA cells, the phosphorylation of AMPK was evaluated. As reported in Figure 3, Panels A and B, AMPK appears hyper-phosphorylated in FA cells with respect to the Wt and FA-corr samples, suggesting that alternative catabolic processes, such as glycolysis, may be stimulated to provide the energy supply in FA cells.

To verify an increase in glycolytic flux linked to the hyper-phosphorylation of AMPK, the activity of HK, PFK and PK were evaluated. As shown in Figure 4 Panels A–C, FA cells display higher activity of these three key glycolytic enzymes compared with control and FA-corr samples. Lactate dehydrogenase (LDH) activity is also increased in FA compared to FA-corr (Figure 4 Panel D), as is lactate release into the medium (Figure 4, Panel E). This increase is fundamental to maintaining cellular homeostasis, because, when OXPHOS is impaired, LDH is the only pathway

able to recycle NADH to NAD<sup>+</sup>. This is confirmed by the evaluation of the basal level of NADH/NAD<sup>+</sup>, which appears similar in all samples (Figure 4, Panel F). On the other hand, when aerobic metabolism has been forced by the addition of DCA or Gal, the NADH/NAD<sup>+</sup> ratio increases in FA cells, but remains stable in Wt and FA-corr cells, confirming that FA cells are unable to recycle NADH through the activity of Complex I (Table II).

To verify the prevalence of glycolytic metabolism in FA cells and the reliability of the results reported above, we measured lactate release, treating the cells with inhibitors of the respiratory chain (Table III). The addition of rotenone causes an increase in lactate production in FA-corr and Wt, but not in FA cells, showing that inhibition of complex I does not change the energy balance in FA cells. Differently, the addition of antimycin A causes increased lactate release in all samples, although it is more evident in FA-corr and Wt cells.

### *3.3 Glutaminolysis does not represent an alternative source of energy production in FA cells.*

Glutaminolysis represents another alternative metabolic pathway to produce energy. In particular, glutamine can be converted to pyruvate, via transaminase activities, or to  $\alpha$ -ketoglutarate, via glutaminase and glutamic dehydrogenase, both molecules involved in aerobic energy metabolism [24].

In FA cells, glutamine metabolism was evaluated by measuring the activity of glutaminase and glutamic dehydrogenase, the main enzymes of this pathway. As shown in Figure 5, the level of these enzymes are lower in FA cells than in Wt and FA-corr cells, suggesting that this pathway is not likely to be involved in sustaining energy metabolism in FA cells.

### *3.4 Constraining FA cells to OXPHOS metabolism represents damage to FA cells*

The altered mitochondrial metabolism in FA cells is associated with increased oxidative stress. In fact, as reported in Figure 6, FA cells display a higher induction of reactive oxygen species (ROS) (Panel A) and increased malondialdehyde (MDA) production (Panel B) compared

with Wt and FA-corr cells. This oxidative stress is also associated with significant mitochondrial membrane depolarisation (MMD; Panel C), which affects the ability of mitochondria to produce ATP. Moreover, drugs used to increase OXPHOS metabolism do not bring benefit to FA cells, but induce increased oxidative stress and MMD. By contrast, DCA and Gal are well tolerated by the Wt and FA-corr samples.

However, DCA treatment induces more negative effects than Gal in FA cells. This could be explained considering that DCA acts on the regulation of PDH activity, forcing the cell to convert most pyruvate into Acetyl CoA. By contrast, galactose is a substrate that induces a respiratory burst, bypassing glycolysis, but allowing pyruvate conversion to lactate, through anaerobic glycolysis.

#### 4. DISCUSSION

This work represents the first systematic exploration of FA energy metabolism. In particular our data show that energy metabolism in FA cells is mainly supported by glycolysis, because aerobic metabolism is impaired by inefficient electron transport through Complex I to Complex III.

However, the enhancement of glycolytic metabolism in FA cells does not appear to adequately satisfy cellular energy requirements, as demonstrated by the low ATP/AMP ratio (Figure 2, Panel C). This is probably due to the low energetic efficiency of glycolysis compared with OXPHOS. By contrast, the increased flux through glycolysis is sufficient to recycle NADH to NAD<sup>+</sup>.

Mitochondrial activity is always correlated with oxidative stress production, which increases when the electron transport chain is not coupled with ATP synthesis [25]. In fact, FA cells are characterised by high levels of oxidative stress [26,27] and appear to be more sensitive to the action of oxidants and GSH depletors [28]. This may depend both on the inefficient electron transport among Complex I and Complex III and on alterations in the mitochondria, which appear swollen with matrix rarefaction [10,13]. Therefore, the high glycolytic flux observed in FA cells may be a strategic attempt by the cells to limit oxidative stress. In fact, when FA cellular metabolism is forced to OXPHOS, the ATP/AMP ratio (Figure 2, Panel C) and the respiration rate (Figure 1,

Panel B) do not improve, and oxidative stress and mitochondrial membrane depolarisation increase (Figure 6). Therefore, on the basis of the data reported in this work, we speculate that the glycolysis enhancement in FA cells may correlate with an activation of the Warburg effect [29]. Indeed our findings appear in direct support of Warburg's central theory.

The inability of FA cells to use aerobic metabolism as their principal energy source, suggests a defective metabolic maturation during the differentiation from haematopoietic stem cell to lymphocyte. In fact, haematopoietic stem cells are characterised, as are all stem cells, by anaerobic metabolism, a distinctive feature to maintain their capacity for self-renewal and pluripotency [30], and switch to aerobic metabolism during differentiation [31]. Therefore, we speculate that the enhanced oxidative stress observed in FA might be relevant in cells attempting a differentiation process [32], suggesting that the mitochondrial impairment is a consequence of the FA genetic defect. Indeed, as elegantly reported by Walter [33], depletion of stem cells derives from an inability of cells bearing a mutation in an FA gene to correct DNA damage induced by haematopoietic stem cells (HSC) exit from dormancy. This tightly links FA phenotypic defects to haematopoietic collapse and BMF. A significant depletion of the CD34+ fraction observed in young FA patients suggests that the FA defect might be associated with a faulty stemness process [34].

## 5. CONCLUSIONS

In conclusion, the maintenance of a glycolytic metabolism remains a signature of the immature condition of FA HSC. As a healthy mitochondrial physiology appears to be a key factor in HSC development, we suggest that the altered mitochondrial physiology in FA is crucial for the depletion of HSC and is associated with BMF and, eventually, cell transformation.



## 6. ACKNOWLEDGEMENTS

We are grateful with the “Cell Line and DNA Biobank from Patients affected by Genetic Diseases” (G. Gaslini Institute) and Telethon Genetic Biobank Network (project no. GTB07001) for the sample providing.

## 7. FUNDING SOURCES

The activity of the Clinical and Experimental Hematology Unit of the G. Gaslini Institut was supported by Fondi 5 x 1000 2013 IRCCS AOU San Martino – IST to PD. AIRFA, ERG spa, Cambiaso and Risso, Rimorchiatori Riuniti, Saar Depositi Oleari Portuali, and UC Sampdoria.

## 8. REFERENCES

- [1] M. Castella, R. Pujol, E. Callén, J.P. Trujillo, J.A. Casado, H. Gille, et al., Origin, functional role, and clinical impact of Fanconi anemia FANCA mutations., *Blood*. 117 (2011) 3759–69. doi:10.1182/blood-2010-08-299917.
- [2] A.D. D’Andrea, M. Grompe, Molecular biology of Fanconi anemia: implications for diagnosis and therapy., *Blood*. 90 (1997) 1725–36.
- [3] A.D. Auerbach, Fanconi anemia and its diagnosis., *Mutat. Res.* 668 (2009) 4–10. doi:10.1016/j.mrfmmm.2009.01.013.
- [4] J. Svahn, C. Dufour, Fanconi anemia - learning from children., *Pediatr. Rep.* 3 Suppl 2 (2011) e8. doi:10.4081/pr.2011.s2.e8.
- [5] P.A. Mehta, J. Tolar, *Fanconi Anemia*, 1993.
- [6] N. V Morgan, A.J. Tipping, H. Joenje, C.G. Mathew, High frequency of large intragenic deletions in the Fanconi anemia group A gene., *Am. J. Hum. Genet.* 65 (1999) 1330–41. doi:10.1086/302627.
- [7] M. Grompe, Fanconi anemia and DNA repair, *Hum. Mol. Genet.* 10 (2001) 2253–2259. doi:10.1093/hmg/10.20.2253.
- [8] W. Du, Z. Adam, R. Rani, X. Zhang, Q. Pang, Oxidative stress in Fanconi anemia hematopoiesis and disease progression., *Antioxid. Redox Signal.* 10 (2008) 1909–21. doi:10.1089/ars.2008.2129.
- [9] E.T. Korthof, J. Svahn, R. Peffault de Latour, P. Terranova, H. Moins-Teisserenc, G. Socié, et al., Immunological profile of Fanconi anemia: a multicentric retrospective analysis of 61 patients., *Am. J. Hematol.* 88 (2013) 472–6. doi:10.1002/ajh.23435.
- [10] S. Ravera, D. Vaccaro, P. Cuccarolo, M. Columbaro, C. Capanni, M. Bartolucci, et al., Mitochondrial respiratory chain Complex I defects in Fanconi anemia complementation group A., *Biochimie.* 95 (2013) 1828–37. doi:10.1016/j.biochi.2013.06.006.

- [11] E. Cappelli, S. Ravera, D. Vaccaro, P. Cuccarolo, M. Bartolucci, I. Panfoli, et al., Mitochondrial respiratory complex I defects in Fanconi anemia., *Trends Mol. Med.* 19 (2013) 513–4. doi:10.1016/j.molmed.2013.07.008.
- [12] G. Cooper, *The Cell: A Molecular Approach.*, second edi, Sunderland (MA), USA, 2000.
- [13] C. Capanni, M. Bruschi, M. Columbaro, P. Cuccarolo, S. Ravera, C. Dufour, et al., Changes in vimentin, lamin A/C and mitofilin induce aberrant cell organization in fibroblasts from Fanconi anemia complementation group A (FA-A) patients., *Biochimie.* 95 (2013) 1838–47. doi:10.1016/j.biochi.2013.06.024.
- [14] M. Filocamo, R. Mazzotti, F. Corsolini, M. Stroppiano, G. Stroppiana, S. Grossi, et al., Cell Line and DNA Biobank From Patients Affected by Genetic Diseases, *Open J. Bioresour.* 1:e2 (2014).
- [15] H. Hanenberg, S.D. Batish, K.E. Pollok, L. Vieten, P.C. Verlander, C. Leurs, et al., Phenotypic correction of primary Fanconi anemia T cells with retroviral vectors as a diagnostic tool., *Exp. Hematol.* 30 (2002) 410–20.
- [16] M. Columbaro, S. Ravera, C. Capanni, I. Panfoli, P. Cuccarolo, G. Stroppiana, et al., Treatment of FANCA Cells with Resveratrol and N-Acetylcysteine: A Comparative Study., *PLoS One.* 9 (2014) e104857. doi:10.1371/journal.pone.0104857.
- [17] M.M. Bradford, A rapid and sensitive method for the quantitation of microgram quantities of protein utilizing the principle of protein-dye binding, *Anal Biochem.* 72 (1976) 248–254.
- [18] S. Ravera, M. Bartolucci, D. Calzia, M.G. Aluigi, P. Ramoino, A. Morelli, et al., Tricarboxylic acid cycle-sustained oxidative phosphorylation in isolated myelin vesicles, *Biochimie.* 95 (2013) 1991–1998. doi:10.1016/j.biochi.2013.07.003.
- [19] S. Ravera, M. Bartolucci, P. Cuccarolo, E. Litamè, M. Illarcio, D. Calzia, et al., Oxidative stress in myelin sheath: The other face of the extramitochondrial oxidative phosphorylation ability., *Free Radic. Res.* (2015) 1–36. doi:10.3109/10715762.2015.1050962.
- [20] J. Kluza, P. Corazao-Rozas, Y. Touil, M. Jendoubi, C. Maire, P. Guerreschi, et al.,

Inactivation of the HIF-1 $\alpha$ /PDK3 signaling axis drives melanoma toward mitochondrial oxidative metabolism and potentiates the therapeutic activity of pro-oxidants., *Cancer Res.* 72 (2012) 5035–47. doi:10.1158/0008-5472.CAN-12-0979.

- [21] C.H. Bauer, B.F. Hassels, W.G. Reutter, Galactose metabolism in regenerating rat liver., *Biochem. J.* 154 (1976) 141–7.
- [22] P.C. Hinkle, P/O ratios of mitochondrial oxidative phosphorylation., *Biochim. Biophys. Acta.* 1706 (2005) 1–11. doi:10.1016/j.bbabi.2004.09.004.
- [23] D. Grahame Hardie, AMP-activated protein kinase: a key regulator of energy balance with many roles in human disease., *J. Intern. Med.* 276 (2014) 543–59. doi:10.1111/joim.12268.
- [24] J. Grooten, The Oxidative Metabolism of Glutamine, *J. Biol. Chem.* 271 (1996) 192–196. doi:10.1074/jbc.271.1.192.
- [25] J. Hroudová, Z. Fišar, Control mechanisms in mitochondrial oxidative phosphorylation., *Neural Regen. Res.* 8 (2013) 363–75. doi:10.3969/j.issn.1673-5374.2013.04.009.
- [26] P. Degan, S. Bonassi, M. De Caterina, L.G. Korkina, L. Pinto, F. Scopacasa, et al., In vivo accumulation of 8-hydroxy-2'-deoxyguanosine in DNA correlates with release of reactive oxygen species in Fanconi's anaemia families., *Carcinogenesis.* 16 (1995) 735–41.
- [27] G. Pagano, A.A. Talamanca, G. Castello, F. V Pallardó, A. Zatterale, P. Degan, Oxidative stress in Fanconi anaemia: from cells and molecules towards prospects in clinical management., *Biol. Chem.* 393 (2012) 11–21. doi:10.1515/BC-2011-227.
- [28] P. Cuccarolo, S. Viaggi, P. Degan, New insights into redox response modulation in Fanconi's anemia cells by hydrogen peroxide and glutathione depletors., *FEBS J.* 279 (2012) 2479–94. doi:10.1111/j.1742-4658.2012.08629.x.
- [29] O. WARBURG, On the origin of cancer cells., *Science.* 123 (1956) 309–14.
- [30] N. Shyh-Chang, G.Q. Daley, L.C. Cantley, Stem cell metabolism in tissue development and aging., *Development.* 140 (2013) 2535–47. doi:10.1242/dev.091777.
- [31] K. Chotinantakul, W. Leeanansaksiri, Hematopoietic stem cell development, niches, and

signaling pathways., Bone Marrow Res. 2012 (2012) 270425. doi:10.1155/2012/270425.

- [32] P. Degan, S. Ravera, E. Cappelli, Why is an energy metabolic defect the common outcome in BMFS?, Cell Cycle. 15 (2016) 2571–2575. doi:10.1080/15384101.2016.1218103.
- [33] D. Walter, A. Lier, A. Geiselhart, F.B. Thalheimer, S. Huntscha, M.C. Sobotta, et al., Exit from dormancy provokes DNA-damage-induced attrition in haematopoietic stem cells, Nature. 520 (2015) 549–52. doi:10.1038/nature14131.
- [34] J.I. Garaycoechea, K.J. Patel, Why does the bone marrow fail in Fanconi anemia?, Blood. 123 (2014) 26–34. doi:10.1182/blood-2013-09-427740.

## 9. TABLES

**Table I: Increased oxygen consumption after the addition of respiratory substrates**

The table shows the oxygen consumption increment after the addition of respiratory substrates. Data are expressed as mean  $\pm$  SD. It can be seen that pyruvate + malate addition does not induce respiration in FA cells, but only in FA-corr and Wt cells. By contrast, succinate induces a greater increase in FA cells with respect to the control samples.

Increment of oxygen consumption

(nmol O/min/mg)

	P/M	Succinate
FA	-1.25 $\pm$ 0.16	9.72 $\pm$ 0.94
FA-corr	9.89 $\pm$ 0.91	5.41 $\pm$ 0.56
Wt	11.06 $\pm$ 1.12	7.06 $\pm$ 0.74

**Table II: Variation of the NADH/NAD<sup>+</sup> ratio after the addition of OXPHOS enhancers.**

The table shows the variation of the NADH/NAD<sup>+</sup> ratio after the addition of OXPHOS enhancers. Data are expressed as mean  $\pm$  SD. It can be seen that both DCA and Gal induce an increase in the NADH/NAD<sup>+</sup> ratio, suggesting NADH accumulation, caused by the impairment of Complex I – Complex III electron transfer. By contrast, negligible alterations were observed in FA-corr and Wt cells.

Variation of NADH/NAD<sup>+</sup>

	DCA	Gal
FA	0.33 $\pm$ 0.40	0.36 $\pm$ 0.04
FA-corr	-0.06 $\pm$ 0.01	0.07 $\pm$ 0.01
Wt	0.06 $\pm$ 0.01	0.03 $\pm$ 0.01

**Table III: Variation of lactate release after the addition of specific OXPHOS inhibitors.**

The table shows increased lactate release after the addition of specific OXPHOS inhibitors. Data are expressed as mean  $\pm$  SD. It can be seen that rotenone, which inhibits Complex I, induces an increase only in FA-corr and Wt cells, confirming the impairment of the Complex I pathway in FA cells. Antimycin A determines increased lactate release in all samples, but it is more evident in FA-corr and Wt cells, suggesting that the mitochondrial metabolism does not play a pivotal role in FA cells energy balance.

Increment of lactate release

(mM Lactate/ $10^6$  cells)

	Rotenone	Antimycin A
FA	$-0.09 \pm 0.01$	$0.35 \pm 0.04$
FA-corr	$0.51 \pm 0.06$	$0.67 \pm 0.06$
Wt	$0.41 \pm 0.05$	$0.54 \pm 0.05$



## 10. FIGURE LEGENDS

**Figure 1: OXPHOS and Krebs cycle activity in FA cells.**

Panel A shows oxygen consumption in the Wt, FA-corr and FA cells. To evaluate the oxygen consumption through the pathway composed by Complexes I, III and IV, 5 mM pyruvate + 2.5 mM malate were added, and afterwards 0.1 mM rotenone was added (P/M + Rot) to inhibit Complex I. To stimulate the pathway composed by Complexes II, III and IV, 10 mM Succinate (Succ) was added and 50  $\mu$ M Antimycin A was added to inhibit Complex III (Succ + Antimyc). The panel is representative of at least five experiments and the data are expressed as mean  $\pm$  SD. \*\*\* and \*\* indicate significant differences for  $p < 0.001$  or  $p < 0.01$ , respectively, between the oxygen consumption induced by respiring substrates and basal respiration. ## indicates a significant difference for  $p < 0.01$  in oxygen consumption in the presence or absence of specific inhibitors. ++ indicates a significant difference for  $p < 0.01$  between the basal respiration of FA cells and the control samples (Wt and FA-corr cell).

Panel B shows the oxygen consumption in Wt, FA-corr and FA cells in the presence of 25 mM dichloroacetate (DCA) or 10 mM galactose (Gal), added to enhance oxidative phosphorylation activity. The panel is representative of at least five experiments and the data are expressed as mean  $\pm$  SD. \*\* indicates a significant difference for  $p < 0.01$ , between the oxygen consumption in the absence of metabolic enhancer and in the presence of DCA or Gal.

Panels C, D and E show, respectively, the activity of three enzymes involved in the Krebs cycle: citrate synthase,  $\alpha$ -ketoglutarate dehydrogenase and fumarase in Wt, FA-corr and FA cells. Each panel is representative of at least five experiments and the data are expressed as mean  $\pm$  SD. No significant differences were observed.

**Figure 2: Energetic status in FA cells**

Panels A and B show the concentrations of ATP and AMP, respectively, in Wt, FA-corr and FA cells, in untreated samples or in the presence of 0.1 mM rotenone (Rot; a specific inhibitor of Complex I), 50  $\mu$ M antimycin A (Antimyc; a specific inhibitor of Complex III), 25 mM dichloroacetate (DCA) or 10 mM galactose (Gal). Panel C shows the ATP/AMP ratio in FA, obtained from the data reported in panels A and B. All three panels are representative of at least five experiments and the data are expressed as mean  $\pm$  SD. \*\* indicates a significant difference between the treated sample and the relative control for  $p < 0.01$ . \* indicates a significant difference between the treated sample and the relative control for  $p < 0.05$ . ++ indicates a significant difference for  $p < 0.01$  between the basal respiration of FA cells and the control samples (Wt and FA-corr cell).

**Figure 3: AMPK phosphorylation in FA cells**

Panel A reports the WB signal against p-AMPK, total AMPK and actin (used as housekeeping proteins) in Wt, FA-corr and FA cells.

Panel B shows densitometric analysis of the WB signal reported in Panel A, normalised versus the actin signal. Each panel is representative of at least five experiments and the data reported in panel B are expressed as mean  $\pm$  SD. \*\* indicates a significant difference for  $p < 0.01$ , between the FA cells and control samples (Wt and FA-corr cells).

**Figure 4: Key glycolytic enzyme activity, lactate release and NADH/NAD<sup>+</sup>**

The figure shows the activity of four key enzymes of anaerobic glycolysis: hexokinase (HK, Panel A), phosphofructokinase (PFK, Panel B), pyruvate kinase (PK, Panel C) and lactate dehydrogenase (LDH, Panel D) in Wt, FA-corr and FA cells. Each panel is representative of at least five experiments and the data are expressed as mean  $\pm$  SD and a significant difference for  $p < 0.01$  between FA cells and the control samples (FA-corr and Wt cells) was observed in each assay.

Panel E shows the medium concentration of lactate released by Wt, FA-corr and FA cells. The panel is representative of at least five experiments and the data are expressed as mean  $\pm$  SD. \*\* indicates a significant difference for  $p < 0.01$  between FA cells and the control samples (FA-corr and Wt cells).

Panel F reports the ratio between the concentration of NADH and NAD<sup>+</sup> in Wt, FA-corr and FA cells. The panel is representative of at least five experiments and the data are expressed as mean  $\pm$  SD. No significant differences were observed.

### **Figure 5: Evaluation of glutaminase and glutamic dehydrogenase activity.**

Panels A and B report the activity of two enzymes involved in glutaminolysis metabolism, glutaminase and glutamic dehydrogenase, in Wt, FA-corr and FA cells, respectively.

Each panel is representative of at least five experiments and the data are expressed as mean  $\pm$  SD.

\*\* indicates a significant difference for  $p < 0.01$ , between the FA cells and control samples (FA-corr and Wt cells).

### **Figure 6: Oxidative stress and mitochondrial membrane depolarisation after treatment with drugs challenging mitochondrial metabolism.**

Panel A reports the ROS induction in Wt, FA-corr and FA cells in untreated samples and in samples treated with 25 mM DCA or 10 mM Gal. Fluorescence was measured using flow cytometry after loading of the cells with H2DCFDA.

Panel B shows the MDA concentration in the untreated samples and in samples treated with 25 mM DCA or 10 mM Gal.

Panel C reports the percentage of mitochondrial membrane depolarisation (MMD) after 24 h of treatment of the cells with 25 mM DCA or 10 mM Gal. MMD was followed by flow cytometry quantification of the treated and untreated cells stained with tetramethyl rhodamine methyl ester (TMRM).

All Panels are representative of at least five experiments and the data are expressed as mean  $\pm$  SD.

\*\* and \* indicate significant differences for  $p < 0.01$  or  $p < 0.05$ , respectively, between the values for untreated samples and cells treated with DCA or Gal.

# # indicates a significant difference for  $p < 0.01$  between the basal values for FA cells and control samples (Wt and FA-corr cell).

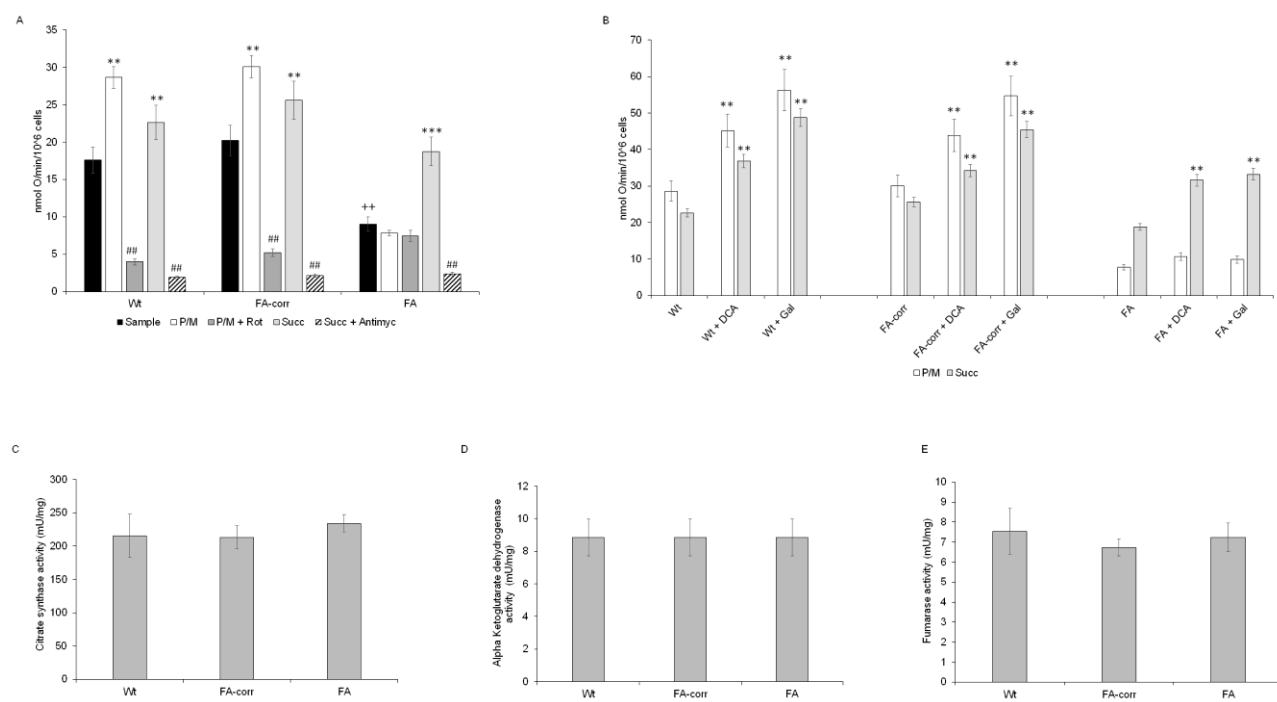


Figure 1

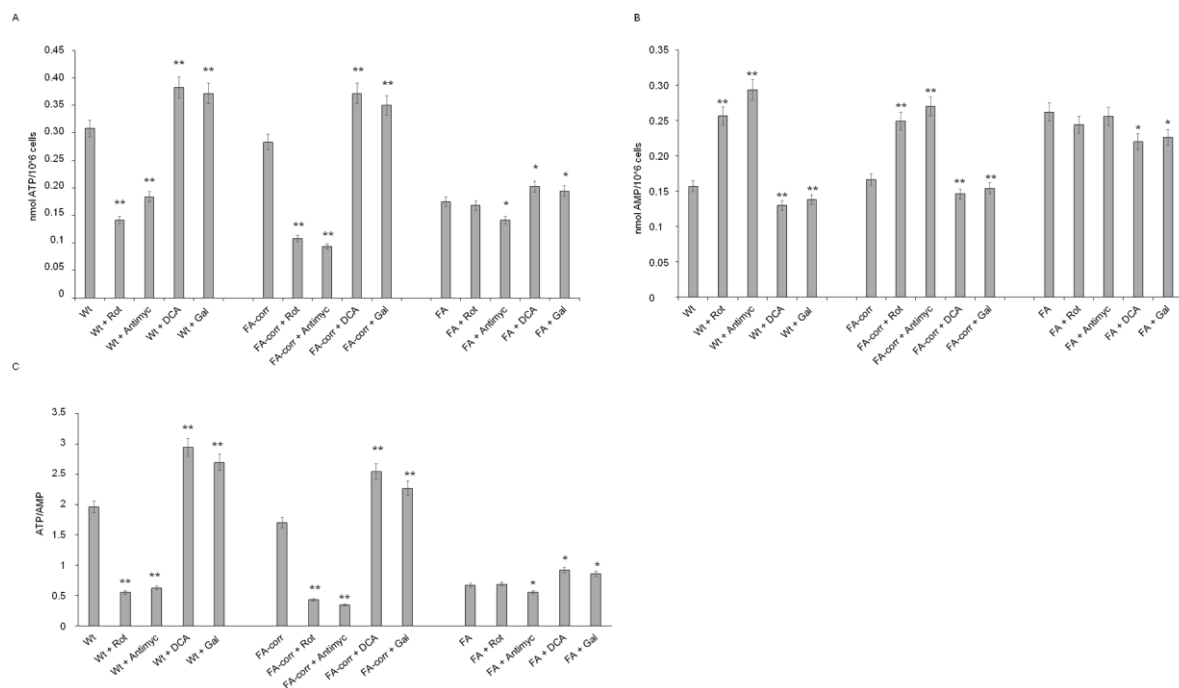
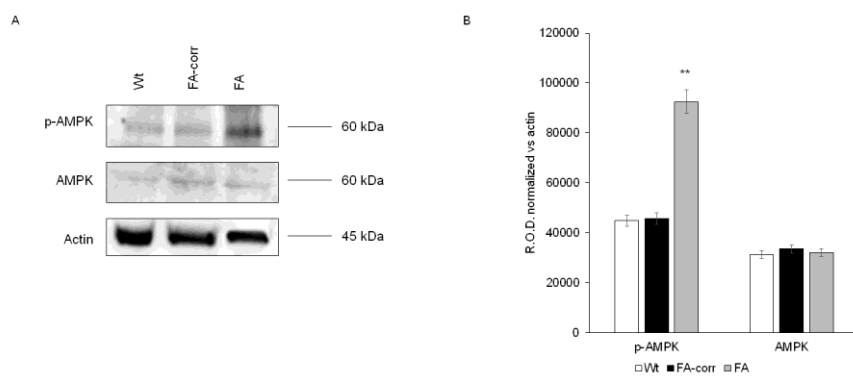


Figure 2



**Figure 3**

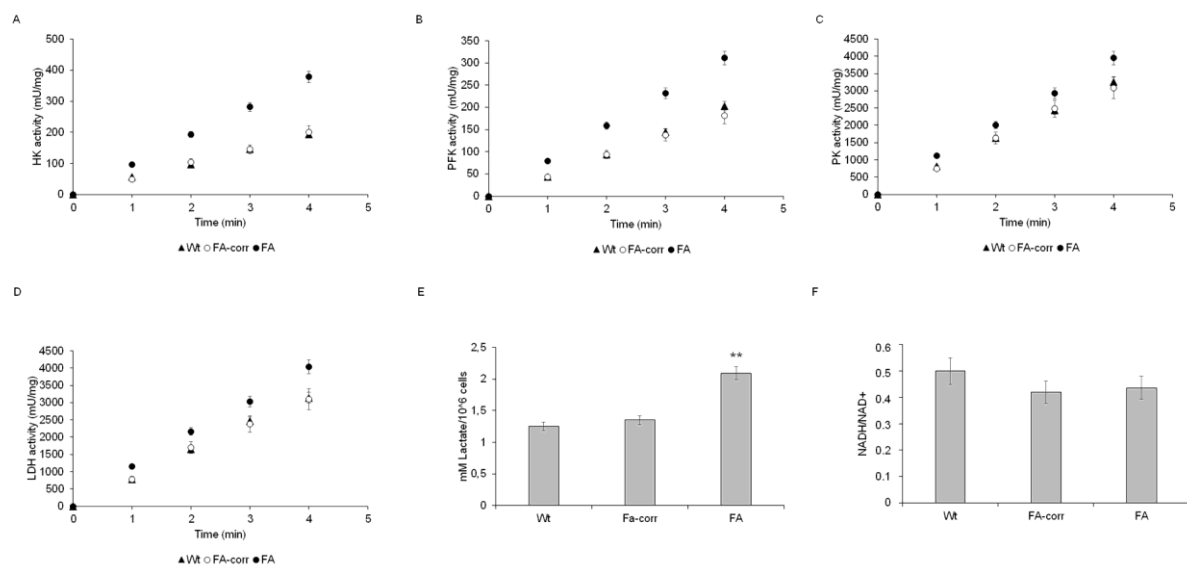


Figure 4



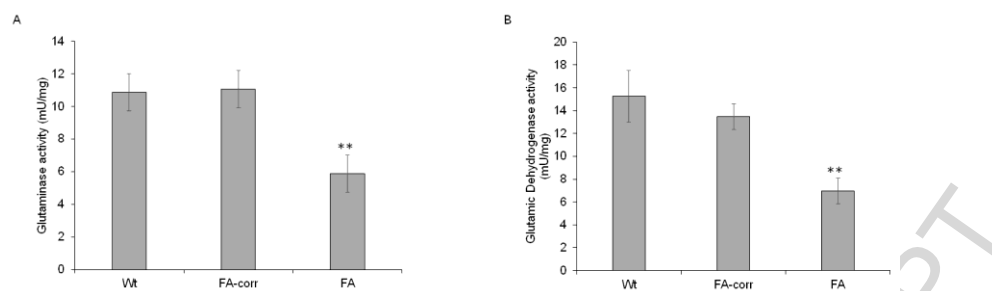


Figure 5

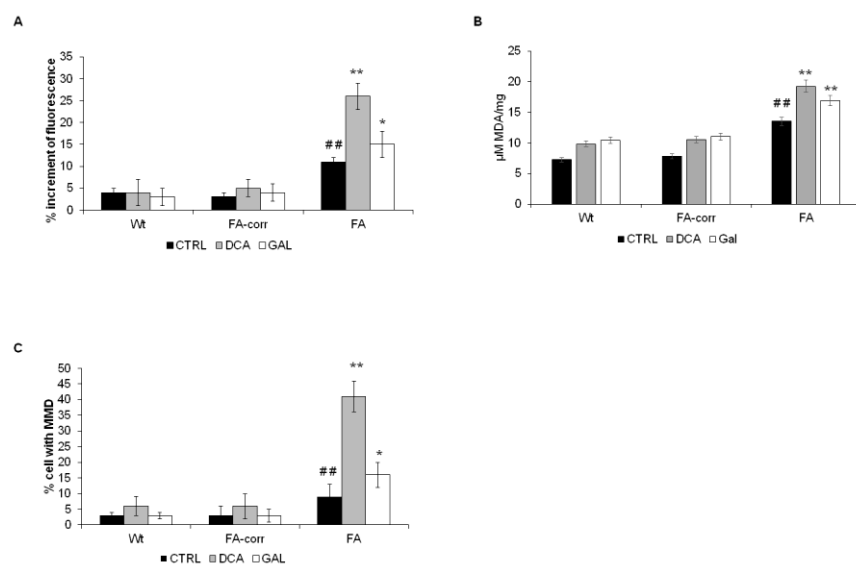


Figure 6

**Highlights**

- Glycolysis is the main pathway to produce energy in Fanconi's anemia cells.
- FA cells display defective mitochondrial functionality with energy deficit
- A forced switch from glycolytic to oxidative metabolism highlights FA cells weakness.